

Constraining baryon annihilation in the hadronic phase of heavy-ion collisions via event-by-event fluctuations

Oleh Savchuk,¹ Volodymyr Vovchenko,² Volker Koch,² Jan Steinheimer,¹ and Horst Stoecker^{1,3,4}

¹*Frankfurt Institute for Advanced Studies, Giersch Science Center,
Ruth-Moufang-Str. 1, D-60438 Frankfurt am Main, Germany*

²*Nuclear Science Division, Lawrence Berkeley National Laboratory, 1 Cyclotron Road, Berkeley, CA 94720, USA*

³*Institut für Theoretische Physik, Goethe Universität Frankfurt,
Max-von-Laue-Str. 1, D-60438 Frankfurt am Main, Germany*

⁴*GSI Helmholtzzentrum für Schwerionenforschung GmbH, Planckstr. 1, D-64291 Darmstadt, Germany*

We point out that the variance of net-baryon distribution normalized by the Skellam distribution baseline, $\kappa_2[B - \bar{B}]/\langle B + \bar{B} \rangle$, is sensitive to the possible modification of (anti)baryon yields due to $B\bar{B}$ annihilation in the hadronic phase. The corresponding measurements can thus place stringent limits on the magnitude of the $B\bar{B}$ annihilation and its inverse reaction. We perform Monte Carlo simulations of the hadronic phase in Pb-Pb collisions at the LHC via the recently developed subensemble sampler + UrQMD afterburner and show that the effect survives in net-proton fluctuations, which are directly accessible experimentally. The available experimental data of the ALICE Collaboration on net-proton fluctuations disfavors a notable suppression of (anti)baryon yields in $B\bar{B}$ annihilations predicted by the present version of UrQMD if only global baryon conservation is incorporated. On the other hand, the annihilations improve the data description when local baryon conservation is imposed. The two effects can be disentangled by measuring $\kappa_2[B + \bar{B}]/\langle B + \bar{B} \rangle$, which at the LHC is notably suppressed by annihilations but virtually unaffected by baryon number conservation.

Introduction. Baryon-antibaryon annihilation is among the most important reactions during the hadronic phase of heavy-ion collisions. With a very large cross section (>60 mb) it has a potentially strong effect on the hadrochemical composition in the final state [1]. The hadronic transport models like UrQMD [2, 3] or SMASH [4] predict sizable suppression of (anti)baryons yields due to the annihilations [5–8]. This provides a possible resolution to the thermal proton yield anomaly at the LHC [9]. However, while the transport models do incorporate the annihilation reactions like $B + \bar{B} \rightarrow n\pi$, the reverse regeneration reactions $n\pi \rightarrow B + \bar{B}$ are presently not implemented, thus violating detailed balance. These reactions can mitigate the effect of annihilations to some extent, if not negate it completely [10–13]. Furthermore, possibilities to explain the thermal proton yield anomaly have been suggested based on reevaluating the chemical equilibrium proton abundances at the conventional chemical freeze-out [14–16].

In this work we present a new way to constrain and quantify the effect of $B\bar{B}$ annihilations on (anti)baryon abundances by utilizing measurements of event-by-event fluctuations. Cumulants of the (net-)(anti)proton distributions have recently been measured in various experiments, including the ALICE Collaboration at the LHC [17], the STAR Collaboration at RHIC [18, 19], and the HADES Collaboration at GSI [20]. These measurements have primarily been motivated to probe the phase structure of QCD, in particular in the hunt for the hypothetical QCD critical point [21, 22]. Here, we point out that specific combinations of first and second moments of baryon (proton) numbers are sensitive to $B\bar{B}$ annihilations.

Annihilations and fluctuations. Let us denote by $\gamma_{B(\bar{B})}$ the modification factors of the mean yields of (anti)baryons during the hadronic phase for a particular collision energy and centrality, i.e.

$$\langle N_{B(\bar{B})}^{\text{fin}} \rangle = \gamma_{B(\bar{B})} \langle N_{B(\bar{B})}^{\text{hyd}} \rangle. \quad (1)$$

$\langle N_{B(\bar{B})}^{\text{fin}} \rangle$ is the final mean yield of (anti)baryons and $\langle N_{B(\bar{B})}^{\text{hyd}} \rangle$ is the mean yield at the beginning of the hadronic phase, i.e. at the end of the hydrodynamic evolution. $\gamma_{B(\bar{B})} = 1$ corresponds to a vanishing net effect of baryon annihilations and regenerations whereas $\gamma_{B(\bar{B})} < 1$ corresponds to a suppression of the yields as observed in transport models.

Instead of the mean, let us consider now the variance $\kappa_2[B - \bar{B}]$ of net baryon distribution. Since the net baryon number is unchanged in $B\bar{B}$ annihilations, or in any other QCD process for that matter, $\kappa_2[B - \bar{B}]$ is unaffected by the hadronic phase evolution, as long as the diffusion of baryons in and out of the acceptance can be neglected:

$$\kappa_2^{\text{fin}}[B - \bar{B}] = \kappa_2^{\text{hyd}}[B - \bar{B}] \quad (2)$$

To obtain an intensive (volume-independent) measure of the net baryon number fluctuations it is convenient to normalize $\kappa_2^{\text{fin}}[B - \bar{B}]$ by the mean number of baryons and antibaryons, $\langle N_B + N_{\bar{B}} \rangle$:

$$R_{B-\bar{B}}^{\text{fin}} \equiv \frac{\kappa_2^{\text{fin}}[B - \bar{B}]}{\langle N_B^{\text{fin}} + N_{\bar{B}}^{\text{fin}} \rangle} = \frac{\kappa_2^{\text{hyd}}[B - \bar{B}]}{\langle \gamma_B N_B^{\text{hyd}} + \gamma_{\bar{B}} N_{\bar{B}}^{\text{hyd}} \rangle}. \quad (3)$$

It follows from Eq. (3) that any suppression of the baryon yields in the hadronic phase ($\gamma_{B(\bar{B})} < 1$) leads to

an enhancement of the normalized net baryon variance. Measurement of such an enhancement is the key idea here to constrain the annihilation.

Fluctuations at the LHC. To isolate the effect of annihilation on $R_{B-\bar{B}}$ other physical mechanisms affecting this quantity must be well controlled. In the limit of uncorrelated baryon production at particlization, as is the case for the ideal hadron resonance gas (HRG) model in the grand-canonical ensemble, the quantity $R_{B-\bar{B}}^{\text{hyd}} = \kappa_2^{\text{hyd}} [B - \bar{B}] / \langle N_B^{\text{hyd}} + N_{\bar{B}}^{\text{hyd}} \rangle$ would be equal to unity. However, it is known from first-principle lattice calculations that cumulants of the baryon number distribution in QCD deviate from this baseline at temperatures $T \sim 150 - 160$ MeV relevant for particlization [23, 24]. Furthermore, baryon number fluctuations in heavy-ion collisions are affected by exact conservation of baryon number [25]. These two issues have recently been addressed in Ref. [26] via a generalized Cooper-Frye particlization routine called *subensemble sampler*. In the following we will employ this sampler to evaluate the effect of $B\bar{B}$ annihilations on experimentally observable event-by-event fluctuations.

We restrict our calculations to 2.76 TeV central Pb-Pb collisions, where measurements of net-proton fluctuations done by the ALICE Collaboration have recently become available [17]. At this high beam energy, the effect of baryon annihilation will be most obvious since baryons and anti-baryons are created in equal amounts. The measurements of the net-particle number variances at the LHC have an additional advantage, since they are unaffected by volume fluctuations [27, 28]. The subensemble sampler of Ref. [26] is used to generate events consisting of hadrons and resonances at particlization, which is assumed to take place at $T = 160$ MeV and $\mu_B = 0$. The procedure incorporates baryon excluded volume effects, matched to lattice QCD data on baryon susceptibilities [29], as well as exact global baryon conservation (see Ref. [26] for the details). The particlization hypersurface incorporates the collective flow [30, 31], taken from the longitudinally boost-invariant blast-wave model [32], which corresponds to a cylinder $r_\perp < r_{\text{max}}$ in the transverse plane at a constant value $\tau = \tau_0$ of the longitudinal proper time. The transverse velocity is parameterized as $\beta_\perp = \beta_s (r_\perp / r_{\text{max}})^n$, with parameters $\beta_s = 0.8$, $r_{\text{max}} = 10$ fm, and $n = 1$ taken from Ref. [33]. The value of $\tau_0 = 11.6$ fm/c is taken to reproduce the effective volume per unit of rapidity $dV/dy \sim 4000$ fm³ at particlization, as suggested by thermal models [15, 34]. We checked that with this choice of parameters the resulting hypersurface accurately reproduces the results of numerical fluid dynamic simulations at the LHC within the UrQMD+hybrid model [35]. To account for the finite longitudinal extent of the system we impose a cut-off $|\eta_s| < 4.8$ on the longitudinal space-time rapidity, which, as shown in Ref. [26], in the boost-invariant scenario accurately reproduces the experimental estimates for the

full acceptance charged multiplicity [36]. This is necessary to properly take into account exact global baryon number conservation.

The sampled hadrons and resonances in each event are then injected into the hadronic afterburner UrQMD. We run UrQMD using two different configurations: (i) the standard configuration implementing $B\bar{B}$ annihilations and (ii) the second configuration where these reactions were switched off. This allows us to establish the two extreme cases: full annihilation without regeneration which maximizes the effect, and no annihilation at all. We additionally consider a scenario (iii), where we neglect the afterburner stage but instead let all resonances produced at particlization decay immediately into final hadrons. This scenario is labeled blast-wave + decays and has been studied in the original work, Ref. [26]. We sample 1.76, 2.4, and 2.4 million events for the scenarios (i), (ii), (iii), respectively.

We first verify that the mean proton multiplicities, as measured by the ALICE experiment are reproduced. Due to the annihilation, the mean number of baryons is suppressed by a factor $\gamma_{B(\bar{B})} = 0.84$, consistent with earlier results [37]. The mean baryon multiplicity remain unchanged during the hadronic phase if annihilations are switched off. The effect of the hadronic rescattering on the transverse momentum spectra of protons, is to increase the mean p_T from $\langle p_T \rangle = 1.14$ GeV/c (blast-wave + decays) to $\langle p_T \rangle = 1.32$ GeV/c (blast-wave + UrQMD with annihilations) and $\langle p_T \rangle = 1.36$ GeV/c (blast-wave + UrQMD without annihilations), improving the agreement with the ALICE data ($\langle p_T \rangle = 1.33 \pm 0.03$ GeV/c [9]) and exhibiting little sensitivity to $B\bar{B}$ annihilations. This is consistent with observations from earlier afterburner studies [8, 38] and mainly due to the abundant baryon+meson scatterings.

Having fixed the mean multiplicity and ensured a realistic momentum distribution, we can now study the effects of annihilation in more detail. From our simulations we can calculate the second order cumulant κ_2 from the momentum integrated event-by-event multiplicities. The resulting ratio $R_{B-\bar{B}} \times \frac{1}{1-\alpha}$ is shown as function of the rapidity acceptance window, $|y| < \Delta Y_{\text{acc}}/2$ in Fig. 1. The additional factor was introduced to remove the effect of global baryon conservation [39], where $\alpha = \Delta Y_{\text{acc}}/9.6$ [26] with 9.6 being the total rapidity width of the system

All presented curves tend to unity for $\Delta Y_{\text{acc}} \rightarrow 0$. This ‘‘poissonization’’ is expected from a thermal system [40] in the $\Delta Y_{\text{acc}} \rightarrow 0$ limit but goes away in the limit of large rapidity acceptance.

In the absence of any annihilation, the corrected $R_{B-\bar{B}}$ exhibits essentially no sensitivity to the afterburner phase as the results from the blast-wave + decays scenario virtually coincide with blast-wave + UrQMD without $B\bar{B}$ annihilation. In this case the corrected scaled variance exhibits a mild decrease with ΔY_{acc} , saturating at the

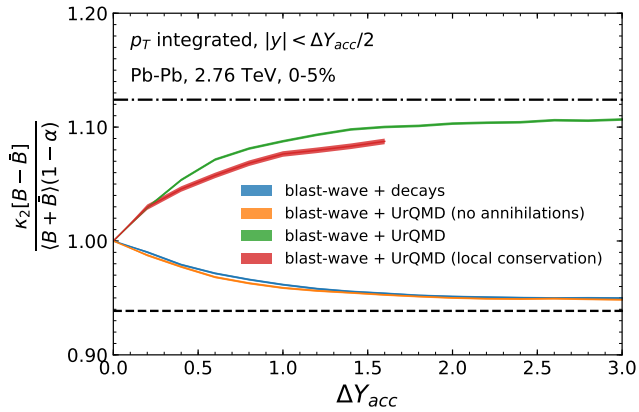


Figure 1. Rapidity acceptance dependence of net baryon $R_{B-\bar{B}} = \kappa_2[B - \bar{B}]/(B + \bar{B})$ in 0-5% central Pb-Pb collisions at the LHC, corrected for baryon number conservation via the $1 - \alpha$ factor. The results are obtained via the subensemble sampler particlization routine applied to the EV-HRG model and blast-wave hypersurface. The different bands correspond to different scenarios for the hadronic phase modeling. The red band corresponds to local baryon conservation in a rapidity range $\Delta y_{\text{cons}} = 3$.

grand canonical value of about 0.94 (dashed line) at $\Delta Y_{\text{acc}} \simeq 1.5$.

When $B\bar{B}$ annihilations are included, the scaled variance exhibits the opposite behavior. As function of ΔY_{acc} , it approaches a value of about 1.12 (dash-dotted line) at large ΔY_{acc} . This ratio at large ΔY_{acc} corresponds to what is expected from Eq. (3) for a reduction of the mean baryon number $R_{B-\bar{B}}^{\text{annih.}}/R_{B-\bar{B}}^{\text{no annih.}} = 0.94/1.12 \simeq 0.84 = \gamma_{B(\bar{B})}$. This sensitivity of $R_{B-\bar{B}}$ at $\Delta Y_{\text{acc}} \gtrsim 1$ to the $B\bar{B}$ -annihilations can be easily understood. While the mean multiplicity is reduced by $\gamma_{B(\bar{B})}$, the second order susceptibility κ_2 remains essentially unchanged. It is straight forward to suggest, that this observable can be used to constrain the quantitative role of baryon annihilation and its back reaction during the hadronic rescattering.

Comparison with experiment. The simulation results on the net proton scaled variance $R_{p-\bar{p}}$ are compared to the available experimental data from the ALICE Collaboration [17] in Figure 2. For this case we assume that protons can only be measured within the ALICE acceptance $0.6 < p < 1.5$ GeV/c for various cuts in longitudinal pseudorapidity $|\eta| < \Delta\eta_{\text{acc}}/2$. Even though the effect of $B\bar{B}$ annihilation in such a reduced acceptance is not as evident as in the p_T integrated net baryon fluctuations discussed above, the observable is still sensitive to annihilations.

We see that for the proton scaled variance, as for the baryons, the results from the blast-wave + decays and blast-wave + UrQMD without $B\bar{B}$ annihilation scenarios virtually coincide. These scenarios are consistent with

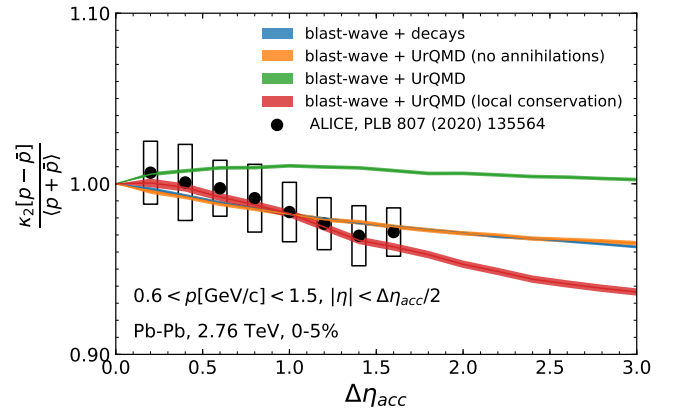


Figure 2. Pseudorapidity acceptance dependence of net proton $R_{p-\bar{p}} = \kappa_2[p - \bar{p}]/(p + \bar{p})$ in 0-5% central Pb-Pb collisions at the LHC. The bands have the same meaning as in Fig. 1. The experimental data of the ALICE collaboration [17] are shown by the symbols with error bars.

the experimental data within errors. Since in this case the effects of global baryon conservation are not corrected, $R_{p-\bar{p}}$ is reduced with increasing acceptance coverage.

When the $B\bar{B}$ annihilations are included (blast-wave + UrQMD), the resulting acceptance dependence notably overestimates the ALICE data, for $\Delta\eta_{\text{acc}} \gtrsim 1$. Therefore, the available experimental data is inconsistent with a notable suppression of (anti)baryon yields in the hadronic phase as predicted by UrQMD in this setup.

Local baryon conservation. However, there is another important property which can effect the scaled variance, namely that baryon number is conserved not only globally but also locally, i.e. in a limited rapidity window. This possibility has been discussed in a previous publication [17]. There it was argued that the data on net-proton fluctuations in central Pb-Pb collisions would favor global over local baryon conservation. The argument for this conclusion was based on the observation that local conservation within $\Delta y_{\text{cons}} \lesssim 5$ units of rapidity, would lead to a stronger suppression of $R_{p-\bar{p}}$ than in the data. However, the analysis in Ref. [17] did not consider the possible effects of $B\bar{B}$ annihilation. As we have shown here, this effect leads to an enhancement of $R_{p-\bar{p}}$ and thus could recover the agreement with the data. It is therefore essential to including annihilation for studying the effects of local conservation.

Several different ways of modeling local baryon conservation have been discussed in the literature [41–47]. We follow the approach of Refs. [42, 45] and incorporate the effect by reducing the space-time rapidity cut-off to $|\eta_s| < \Delta y_{\text{cons}}/2$, where Δy_{cons} is the range of the local baryon conservation in longitudinal rapidity. We take the value $\Delta y_{\text{cons}} = 3$, which was earlier used in Ref. [45] for describing the hadron yields in small systems at the LHC

in the framework of the canonical statistical model.

The calculations including local baryon conservation for $R_{B-\bar{B}}$ (0.4 million events) are shown in Figs. 1 and 2 as red band. These calculations include $B\bar{B}$ annihilations during the hadronic phase. In Fig. 1 the correction for baryon conservation is performed via the $1 - \alpha$ factor where $\alpha = \Delta Y_{\text{acc}}/3$. It is seen that the corrected $R_{B-\bar{B}}$ essentially coincides with the result of global conservation within the conservation radius $\Delta Y_{\text{acc}} < 1.5$. Thus, if the range of baryon conservation is known, the appropriately corrected $R_{B-\bar{B}}$ can be used to constrain the baryon annihilation.

If the conservation range is not independently known, however, the picture is quite different. The combined effect of local baryon conservation and $B\bar{B}$ annihilations on $R_{p-\bar{p}}$ in the ALICE acceptance is shown by the red band in Fig. 2. In this scenario, the calculation with local conservation and annihilation is in good agreement with the experimental data. In the absence of $B\bar{B}$ annihilations the data would be notably underestimated due to local conservation, as shown in Ref. [17], however when both the local conservation and $B\bar{B}$ annihilation are implemented simultaneously, the agreement with the data is recovered.

Distinguishing annihilation from local baryon conservation. The data presented by the ALICE collaboration currently does not allow us to distinguish global conservation without $B\bar{B}$ annihilations from local conservation with $B\bar{B}$ annihilations, although it can be argued that the shape of $\Delta\eta_{\text{acc}}$ dependence is better reproduced by the latter scenario. Additional analysis is required to answer this question more definitively and also possibly put quantitative constraints on the effect of annihilation and regeneration during the hadronic phase.

One option is to look into the centrality dependence of $R_{p-\bar{p}}$. The effect of the hadronic phase (and thus $B\bar{B}$ annihilations) decreases for larger impact parameter, and can basically be neglected in peripheral collisions. Experimental data on $R_{p-\bar{p}}$ [17] do indicate a centrality dependence: $R_{p-\bar{p}}$ decreases from 0.972 ± 0.015 in 0-5% central collisions to 0.935 ± 0.011 in 60-70% central collisions. The latter value was shown in Ref. [45] to be consistent with local baryon conservation with $\Delta y_{\text{cons}} = 3$ without $B\bar{B}$ annihilations. If (local) baryon conservation is independent of centrality, for instance if it is determined by the quark-anti-quark creation in the early stage of the collision, the centrality dependence of the data favors the local conservation + $B\bar{B}$ annihilation scenario. Additional support for this scenario can be found in the centrality dependence of the p/π ratio, where the data show indications for suppression in central Pb-Pb collisions [9], consistent with the effect of $B\bar{B}$ annihilations.

Besides these indications, another observable which is able to distinguish these two scenarios, based on experimental data, would be very useful. To disentangle the local baryon conservation from $B\bar{B}$ annihilation

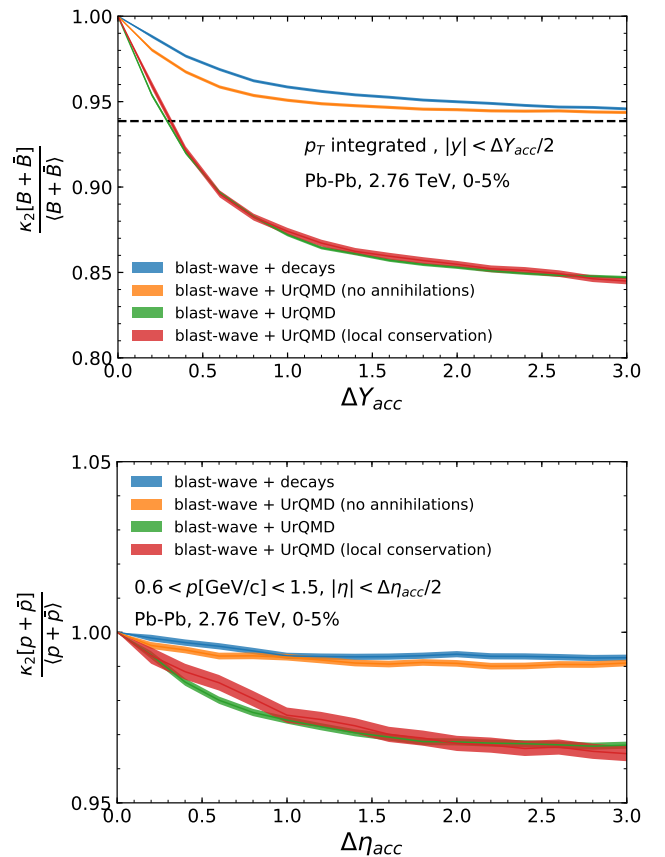


Figure 3. (a) Rapidity acceptance dependence of net baryon $R_{B+\bar{B}} = \kappa_2[B+\bar{B}]/(B+\bar{B})$ in 0-5% central Pb-Pb collisions at the LHC. The different bands have the same meaning as in Fig. 1. (b) Same as Fig. 2 but for $R_{p+\bar{p}}$. The calculations shown in this figure are not corrected for volume fluctuations.

tions more directly we propose to study an additional fluctuation measure. In particular the scaled variance $R_{B+\bar{B}} \equiv \kappa_2[B+\bar{B}]/\langle N_B + N_{\bar{B}} \rangle$ [or $R_{p+\bar{p}}$ for protons] of the total baryon (proton) + antibaryon (antiproton) number can be used for this purpose. This quantity is not sensitive to baryon conservation at the LHC because its correlator with the conserved net baryon number vanishes due to symmetry:

$$\text{cov}[B+\bar{B}, B-\bar{B}] = \text{cov}[B, B] - \text{cov}[\bar{B}, \bar{B}] \stackrel{\langle B \rangle = \langle \bar{B} \rangle}{=} 0. \quad (4)$$

However, $R_{B+\bar{B}}$ is sensitive to the annihilation and thus can be used to constrain this effect. Figure 3 shows the results of calculations for (a) $R_{B+\bar{B}}$ as function of the rapidity acceptance ΔY_{acc} and (b) $R_{p+\bar{p}}$ as function of the pseudorapidity acceptance $\Delta\eta_{\text{acc}}$ within the ALICE momentum acceptance $0.6 < p < 1.5$ GeV/c. The numerical results explicitly illustrate that these two quantities are not sensitive to baryon number conservation: in the absence of $B\bar{B}$ annihilations $R_{B+\bar{B}}$ approaches the

grand-canonical value for large ΔY_{acc} whereas the calculations with the annihilations that incorporate either global or local baryon conservation yield identical results. The effect of $B\bar{B}$ annihilations is to suppress both quantities. In particular, the suppression is notable for $R_{p+\bar{p}}$ within the ALICE acceptance, thus the measurements can in principle be used to study $B\bar{B}$ annihilations independent of the (local) baryon conservation.

Note that, in contrast to the net charges, $R_{p+\bar{p}}$ is significantly affected by volume fluctuations even at the LHC. The calculations in Fig. 3 do not incorporate volume fluctuations, thus, for a meaningful comparison either the data have to be corrected for volume fluctuations or volume fluctuations included in the model calculation. The data can be corrected using models for volume fluctuations, for example the Glauber Monte Carlo [28]. We have checked that the errors for $R_{p+\bar{p}}$ that can be derived from the published data on proton fluctuations [17], as well as the systematic errors from performing the correction for volume fluctuations are presently too large to distinguish the difference between the annihilation scenarios shown in Fig. 3. However, this should be possible with upcoming high precision data. The event-by-event fluctuations presented here will also be useful in the ongoing efforts to properly implement the regeneration reactions in hadronic afterburners.

Summary. We pointed out for the first time that measurements of event-by-event fluctuations in heavy-ion collisions can be used to quantify the effect of baryon annihilation in the hadronic phase. The key observation is that the combined measurement of the scaled variance of the net and total proton + anti-proton number can be used to strictly constrain the role of baryon – anti-baryon annihilation during the hadronic phase of heavy ion collisions at the LHC. Including only annihilation, without any regeneration, enhances appreciably the scaled variances of the net baryon and net proton distributions. A direct comparison with experimental data from the ALICE experiment leads to two possible scenarios which both equally well describe the data. Either, baryons are completely regenerated and baryon number is conserved only globally or, the mean baryon number is reduced due to annihilation which requires a more local conservation of the baryon number. In particular if one neglects the effects of baryon pair regeneration in the hadronic phase a conservation radius of $\Delta y_{\text{cons}} = 3$ units in rapidity is observed. To distinguish these two scenarios we suggest a new observable: the scaled variance of the number of protons + anti-protons, which shows a clearly distinguished dependence on annihilation and local conservation. With a simultaneous observation of these two quantities one could finally experimentally establish the quantitative effect of annihilation during the hadronic phase.

Acknowledgments. This work received support through the U.S. Department of Energy, Office of Science, Office of Nuclear Physics, under contract number DE-

AC02-05CH11231231 and within the framework of the Beam Energy Scan Theory (BEST) Topical Collaboration. V.V. acknowledges the support through the Feodor Lynen program of the Alexander von Humboldt foundation. J.S. thank the Samson AG and the BMBF through the ErUMData project for funding. H.St. acknowledges the Walter Greiner Gesellschaft zur Förderung der physikalischen Grundlagenforschung e.V. through the Judah M. Eisenberg Laureatus Chair at Goethe Universität Frankfurt am Main.

-
- [1] S. A. Bass and A. Dumitru, *Phys. Rev. C* **61**, 064909 (2000), [arXiv:nucl-th/0001033](#).
 - [2] S. A. Bass *et al.*, *Prog. Part. Nucl. Phys.* **41**, 255 (1998), [arXiv:nucl-th/9803035](#).
 - [3] M. Bleicher *et al.*, *J. Phys. G* **25**, 1859 (1999), [arXiv:hep-ph/9909407](#).
 - [4] J. Weil *et al.*, *Phys. Rev. C* **94**, 054905 (2016), [arXiv:1606.06642 \[nucl-th\]](#).
 - [5] F. Becattini, M. Bleicher, T. Kollegger, M. Mitrovski, T. Schuster, and R. Stock, *Phys. Rev. C* **85**, 044921 (2012), [arXiv:1201.6349 \[nucl-th\]](#).
 - [6] J. Steinheimer, J. Aichelin, and M. Bleicher, *Phys. Rev. Lett.* **110**, 042501 (2013), [arXiv:1203.5302 \[nucl-th\]](#).
 - [7] F. Becattini, M. Bleicher, T. Kollegger, T. Schuster, J. Steinheimer, and R. Stock, *Phys. Rev. Lett.* **111**, 082302 (2013), [arXiv:1212.2431 \[nucl-th\]](#).
 - [8] D. Oliinychenko, L.-G. Pang, H. Elfner, and V. Koch, *Phys. Rev. C* **99**, 044907 (2019), [arXiv:1809.03071 \[hep-ph\]](#).
 - [9] B. Abelev *et al.* (ALICE), *Phys. Rev. C* **88**, 044910 (2013), [arXiv:1303.0737 \[hep-ex\]](#).
 - [10] R. Rapp and E. V. Shuryak, *Phys. Rev. Lett.* **86**, 2980 (2001), [arXiv:hep-ph/0008326](#).
 - [11] Y. Pan and S. Pratt, (2012), [arXiv:1210.1577 \[nucl-th\]](#).
 - [12] Y. Pan and S. Pratt, *Phys. Rev. C* **89**, 044911 (2014).
 - [13] E. Seifert and W. Cassing, *Phys. Rev. C* **97**, 044907 (2018), [arXiv:1801.07557 \[hep-ph\]](#).
 - [14] P. Alba, V. Vovchenko, M. I. Gorenstein, and H. Stoecker, *Nucl. Phys. A* **974**, 22 (2018), [arXiv:1606.06542 \[hep-ph\]](#).
 - [15] V. Vovchenko, M. I. Gorenstein, and H. Stoecker, *Phys. Rev. C* **98**, 034906 (2018a), [arXiv:1807.02079 \[nucl-th\]](#).
 - [16] A. Andronic, P. Braun-Munzinger, B. Friman, P. M. Lo, K. Redlich, and J. Stachel, *Phys. Lett. B* **792**, 304 (2019), [arXiv:1808.03102 \[hep-ph\]](#).
 - [17] S. Acharya *et al.* (ALICE), *Phys. Lett. B* **807**, 135564 (2020), [arXiv:1910.14396 \[nucl-ex\]](#).
 - [18] J. Adam *et al.* (STAR), *Phys. Rev. C* **102**, 024903 (2020), [arXiv:2001.06419 \[nucl-ex\]](#).
 - [19] M. Abdallah *et al.* (STAR), (2021), [arXiv:2101.12413 \[nucl-ex\]](#).
 - [20] J. Adamczewski-Musch *et al.* (HADES), *Phys. Rev. C* **102**, 024914 (2020), [arXiv:2002.08701 \[nucl-ex\]](#).
 - [21] M. A. Stephanov, K. Rajagopal, and E. V. Shuryak, *Phys. Rev. D* **60**, 114028 (1999), [arXiv:hep-ph/9903292](#).
 - [22] A. Bzdak, S. Esumi, V. Koch, J. Liao, M. Stephanov, and N. Xu, *Phys. Rept.* **853**, 1 (2020), [arXiv:1906.00936 \[nucl-th\]](#).

- [23] A. Bazavov *et al.*, *Phys. Rev. D* **95**, 054504 (2017), [arXiv:1701.04325 \[hep-lat\]](#).
- [24] S. Borsanyi, Z. Fodor, J. N. Guenther, S. K. Katz, K. K. Szabo, A. Pasztor, I. Portillo, and C. Ratti, *JHEP* **10**, 205 (2018), [arXiv:1805.04445 \[hep-lat\]](#).
- [25] A. Bzdak, V. Koch, and V. Skokov, *Phys. Rev. C* **87**, 014901 (2013), [arXiv:1203.4529 \[hep-ph\]](#).
- [26] V. Vovchenko and V. Koch, *Phys. Rev. C* **103**, 044903 (2021), [arXiv:2012.09954 \[hep-ph\]](#).
- [27] V. Skokov, B. Friman, and K. Redlich, *Phys. Rev. C* **88**, 034911 (2013), [arXiv:1205.4756 \[hep-ph\]](#).
- [28] P. Braun-Munzinger, A. Rustamov, and J. Stachel, *Nucl. Phys. A* **960**, 114 (2017), [arXiv:1612.00702 \[nucl-th\]](#).
- [29] V. Vovchenko, A. Pasztor, Z. Fodor, S. D. Katz, and H. Stoecker, *Phys. Lett. B* **775**, 71 (2017), [arXiv:1708.02852 \[hep-ph\]](#).
- [30] P. J. Siemens and J. O. Rasmussen, *Phys. Rev. Lett.* **42**, 880 (1979).
- [31] H. Stoecker, A. A. Ogloblin, and W. Greiner, *Z. Phys. A* **303**, 259 (1981).
- [32] E. Schnedermann, J. Sollfrank, and U. W. Heinz, *Phys. Rev. C* **48**, 2462 (1993), [arXiv:nucl-th/9307020](#).
- [33] P. Huovinen, P. M. Lo, M. Marczenko, K. Morita, K. Redlich, and C. Sasaki, *Phys. Lett. B* **769**, 509 (2017), [arXiv:1608.06817 \[hep-ph\]](#).
- [34] A. Andronic, P. Braun-Munzinger, K. Redlich, and J. Stachel, *Nature* **561**, 321 (2018), [arXiv:1710.09425 \[nucl-th\]](#).
- [35] H. Petersen, J. Steinheimer, G. Burau, M. Bleicher, and H. Stöcker, *Phys. Rev. C* **78**, 044901 (2008), [arXiv:0806.1695 \[nucl-th\]](#).
- [36] E. Abbas *et al.* (ALICE), *Phys. Lett. B* **726**, 610 (2013), [arXiv:1304.0347 \[nucl-ex\]](#).
- [37] F. Becattini, J. Steinheimer, R. Stock, and M. Bleicher, *Phys. Lett. B* **764**, 241 (2017), [arXiv:1605.09694 \[nucl-th\]](#).
- [38] J. Steinheimer, J. Aichelin, M. Bleicher, and H. Stöcker, *Phys. Rev. C* **95**, 064902 (2017), [arXiv:1703.06638 \[nucl-th\]](#).
- [39] M. Bleicher, S. Jeon, and V. Koch, *Phys. Rev. C* **62**, 061902 (2000), [arXiv:hep-ph/0006201](#).
- [40] B. Ling and M. A. Stephanov, *Phys. Rev. C* **93**, 034915 (2016), [arXiv:1512.09125 \[nucl-th\]](#).
- [41] P. Castorina and H. Satz, *Int. J. Mod. Phys. E* **23**, 1450019 (2014), [arXiv:1310.6932 \[hep-ph\]](#).
- [42] V. Vovchenko, B. Dönigus, and H. Stoecker, *Phys. Lett. B* **785**, 171 (2018b), [arXiv:1808.05245 \[hep-ph\]](#).
- [43] D. Oliinychenko and V. Koch, *Phys. Rev. Lett.* **123**, 182302 (2019), [arXiv:1902.09775 \[hep-ph\]](#).
- [44] C. A. Pruneau, *Phys. Rev. C* **100**, 034905 (2019), [arXiv:1903.04591 \[nucl-th\]](#).
- [45] V. Vovchenko, B. Dönigus, and H. Stoecker, *Phys. Rev. C* **100**, 054906 (2019), [arXiv:1906.03145 \[hep-ph\]](#).
- [46] P. Braun-Munzinger, A. Rustamov, and J. Stachel, (2019), [arXiv:1907.03032 \[nucl-th\]](#).
- [47] I. Altsybeev, (2020), [arXiv:2002.11398 \[nucl-th\]](#).